Supplementary Information:

Incorporating Spectroscopic On-line Monitoring as a Method of Detection for a Lewis Cell Setup

Forrest D. Heller[a,b], Amanda J. Casella[a], Gregg J. Lumetta[a], Kenneth L. Nash[b], Sergey I. Sinkov[a] and Samuel A. Bryan[a]

Figure 1: Overview of Lewis cell setup

Calibration Data:

The UV-Vis probe was calibrated for real time monitoring by checking the spectroscopy for the lanthanides (praseodymium, neodymium, europium, samarium, holmium, and erbium) planned for future use. As a comparison to the literature the lanthanides of interest were first spectro-titrated in solutions of DI water. From this data, Beer's law plots were drawn using a representative peak. Note that the optical path length for the UV-Vis probes is 2.5 cm.

[a.] Pacific Northwest National Laboratory, Energy and Environment Directorate,
Pacific Northwest National Laboratory, Richland, WA 99352 USA

[b.] Washington State University, Department of Chemistry, PO Box 644630
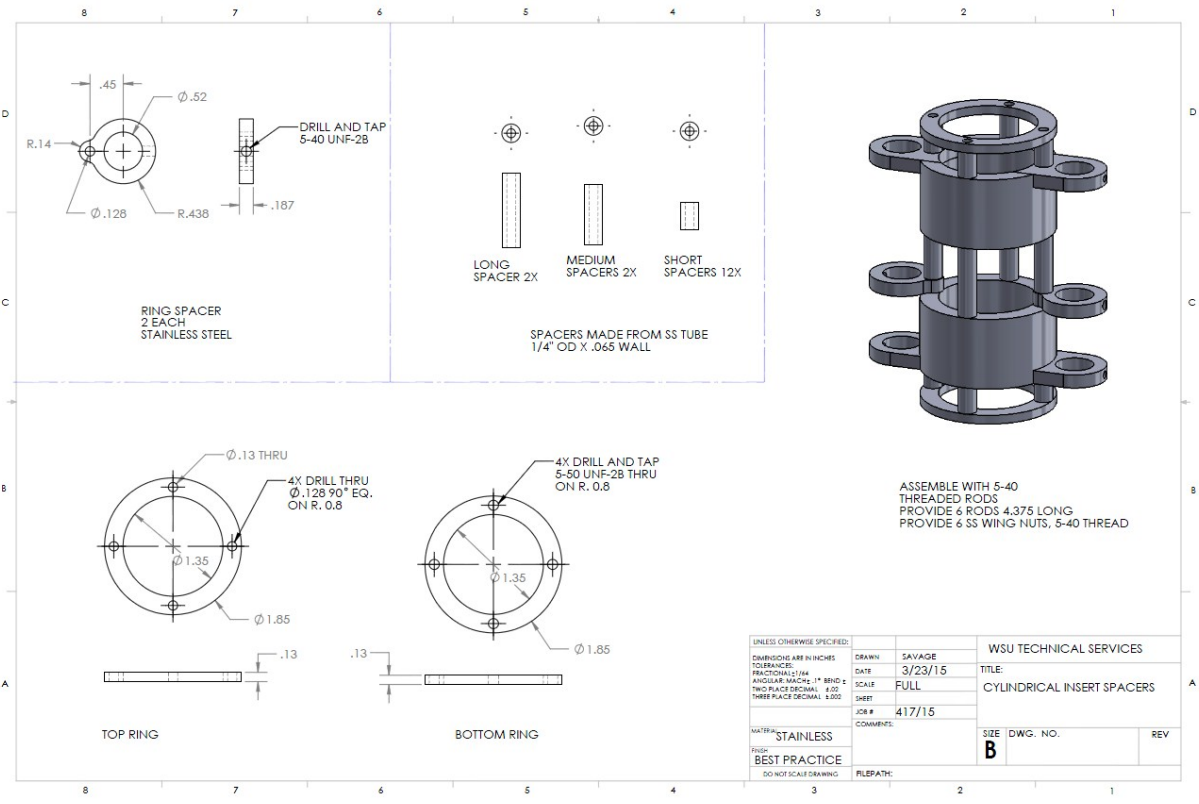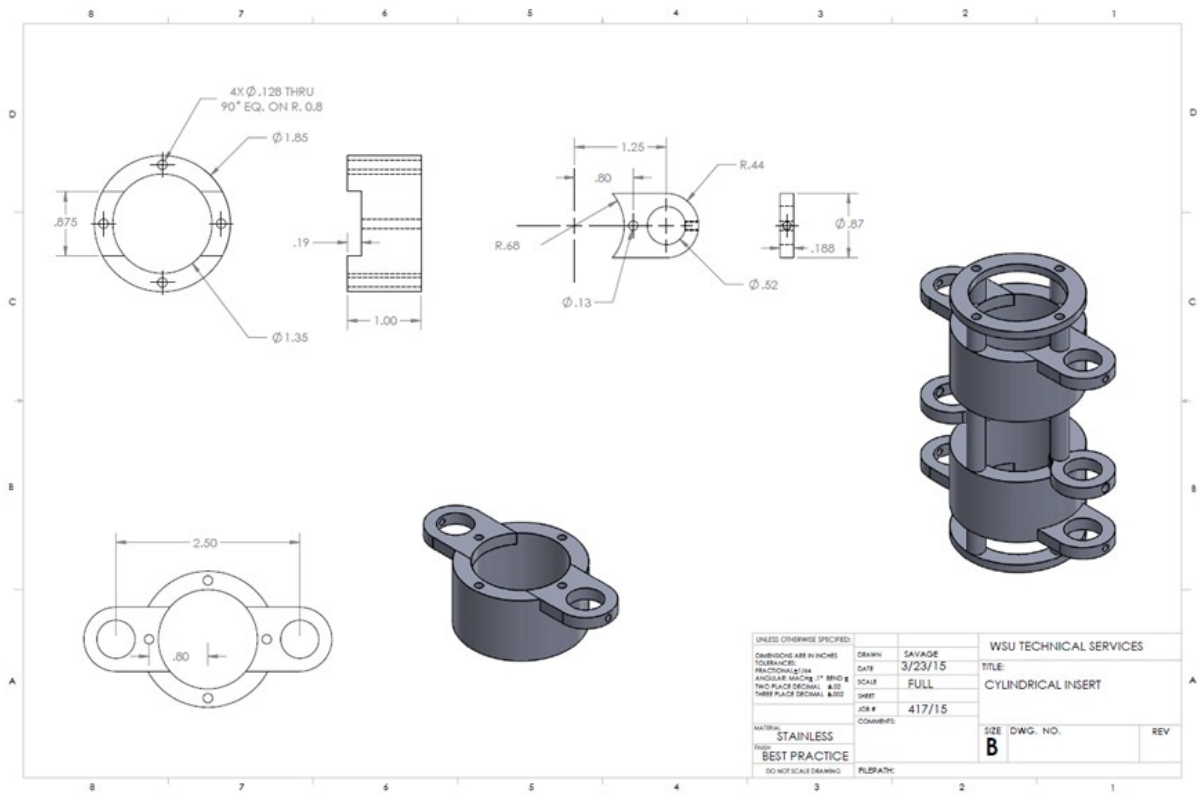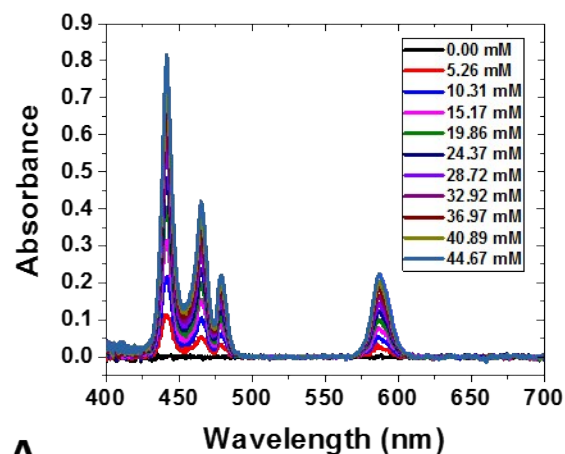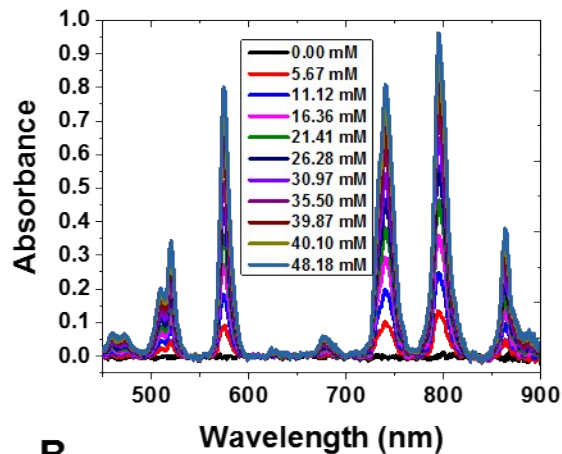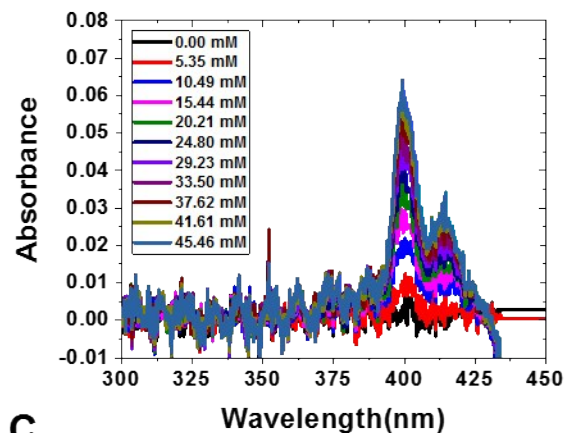Pullman, WA 99164-4630 USA

Figure 2: Cylindrical Insert Blueprints provided by the Washington State University Instrument Shop for the machining of the cylindrical inserts

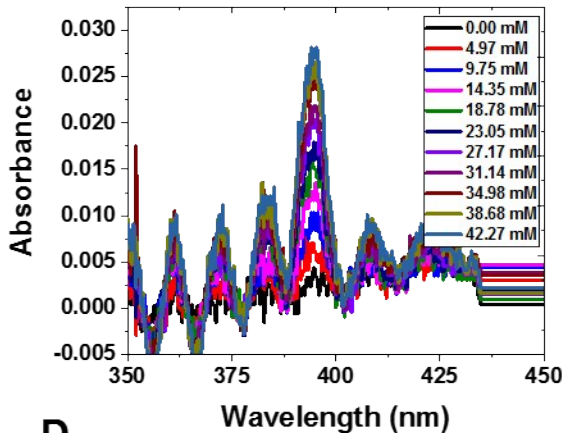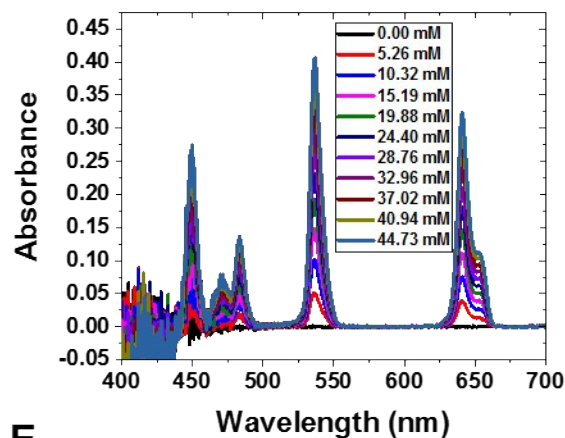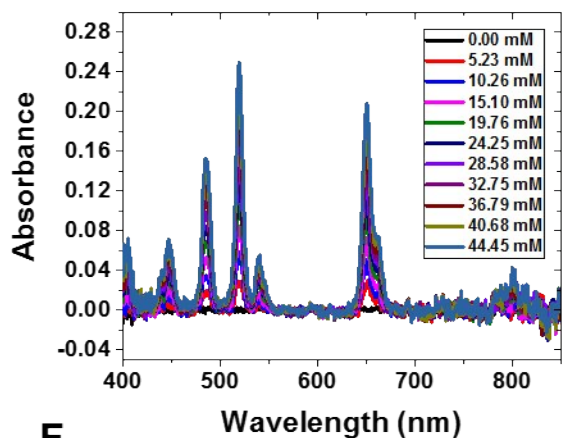Figure 3: Spectra of lanthanides A) Pr(NO$_3$)$_3$ B) Nd(NO$_3$)$_3$ C) Eu(NO$_3$)$_3$ D) Sm(NO$_3$)$_3$ E) Ho(NO$_3$)$_3$ F) Er(NO$_3$)$_3$ in DI water.

Table 1: Molar absorptivity values calculated from Beer's law plots of representative wavelengths for each lanthanide nitrate in DI water compared to the values from Carnall[1]. Error is calculated using propagation of error from the uncertainty of the Beer's law plot slope.

Metal	Wavelength (nm)	Calculated Extinction Coefficient $(M^{-1}*cm^{-1})$	Literature Extinction Coefficient $(M^{-1}*cm^{-1})$
Praseodymium	443	7.23 (±0.15)	10.4
Neodymium	794	7.92 (±0.13)	12.5
Samarium	399	0.532 (±0.024)	3.31
Europium	394	0.241 (±0.009)	2.77
Holmium	449	2.44 (±0.059)	3.90
Erbium	519	2.32 (±0.015)	3.40

Because of the complexing nature of the aqueous phase components which affect the absorbance spectra, it was necessary to do a calibration for the lanthanide metals of interest in solution environments similar to that of the planned experiments. One example is the largest peak around 450 nm for holmium whose molar absorptivity changes greatly when in the presence of citric acid and HEDTA. For the extraction aqueous phase solutions of 0.6 M citric acid, 0.125 M HEDTA and lanthanide at pH 2.52 were made. The solutions were made a series of batches with lanthanide concentrations in increments of 5 mM from 0 mM to 25 mM lanthanide. From the spectra of each lanthanide a Beer's law plot was drawn for a representative wavelength. Once again these were done with a path length of 2.5 cm.
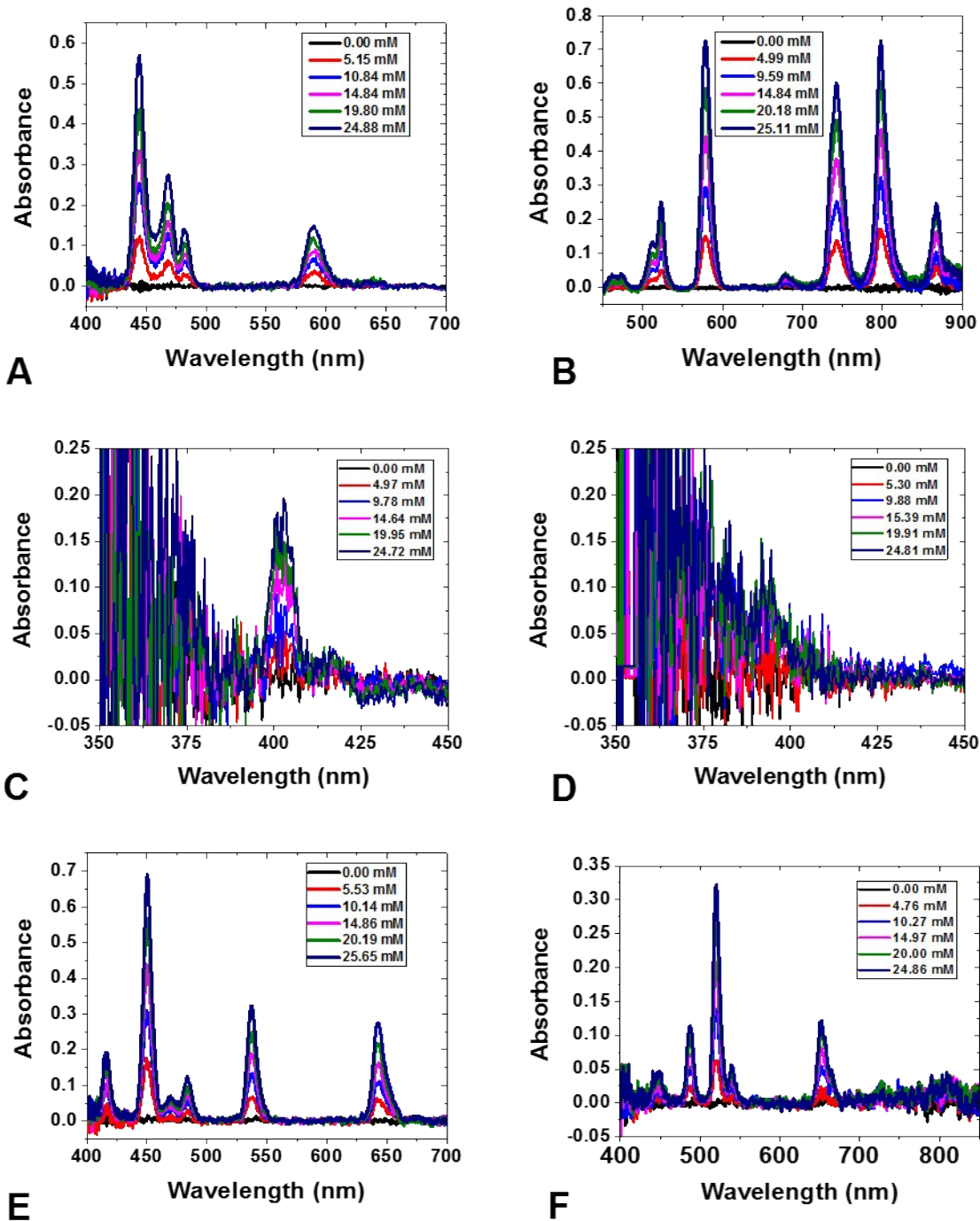
Figure 4: Spectra of lanthanides A) Pr(NO$_3$)$_3$ B) Nd(NO$_3$)$_3$ C) Sm(NO$_3$)$_3$ D) Eu(NO$_3$)$_3$ E) Ho(NO$_3$)$_3$ F) Er(NO$_3$)$_3$ in aqueous phase. Aqueous phase consisting of 0.6 M citric acid and 0.125 M HEDTA adjusted to pH 2.52.

Table 2: Molar absorptivity values calculated from Beer's Law plots of representative wavelengths for each lanthanide nitrate in aqueous phase. Aqueous phase consisting of 0.6 M citric acid and 0.125 M HEDTA adjusted to pH 2.52. Europium is not shown as the absorptivity values were too weak to yield reliable calibration curves. Error is calculated using propagation of error from the uncertainty of the Beer's law plot slope.

Metal	Wavelength (nm)	Extinction Coefficient ($M^{-1}*cm^{-1}$)
Praseodymium	444	9.03 (±0.40)
Neodymium	798	11.4 (±0.4)
Samarium	403	2.86 (±0.16)
Holmium	450	10.6 (±0.2)
Erbium	520	5.33 (±0.11)

To test the spectra in the organic phase several batches of aqueous and organic phases were made. For the aqueous phase two blank 0 mM lanthanide batches were made plus a 50 mM and a 75 mM lanthanide nitrate batch were made. Each aqueous phase was 0.6 M citric acid and 0.125 M HEDTA at pH 2.52. For every aqueous phase that was made a 0.25 M HEH[EHP] in n-dodecane organic phase batch solution was prepared. Before contacting, the UV-Vis spectra of each organic and aqueous phase were taken. After 30 minutes of vigorous mixing of the two phases, the aqueous and organic phases were separated by centrifugation and each phase's spectrum was taken again. These before and after spectra allowed the lanthanide concentration in the organic phase to be calculated using the below equation:

$$[Ln_{org}] = [Ln_{aqi}] - \frac{A_{aqi} - A_{aqf}}{A_{aqi}} \cdot [Ln_{aqi}] \quad (1)$$

Each loaded organic phase was fractionally mixed with the blank organic phase so that they formed a series of organic solutions that ranged from blank to fully loaded organic phase as shown in Table 3.

Table 3: Solution table for preparing organic phase for spectroscopic measurement

Fraction of Loaded/Blank Phase	Blank Org Phase (mL)	Loaded Org Phase (mL)
0:15	15	0
3:12	12	3
6:9	9	6
9:6	6	9
12:3	3	12
15:0	0	15

The UV-Vis spectra of this fractionated series of solutions were taken to form a Beer's law plot for each lanthanide in the organic phase. For some lanthanides the organic phase molar absorptivity values are significantly smaller than equivalent peaks in aqueous phase. For this reason there were no usable absorbance peaks for europium and samarium and thus no Beer's law plots for those lanthanides were made. Once again it is worth noting that all these spectra had an optical path length of 2.5 cm.
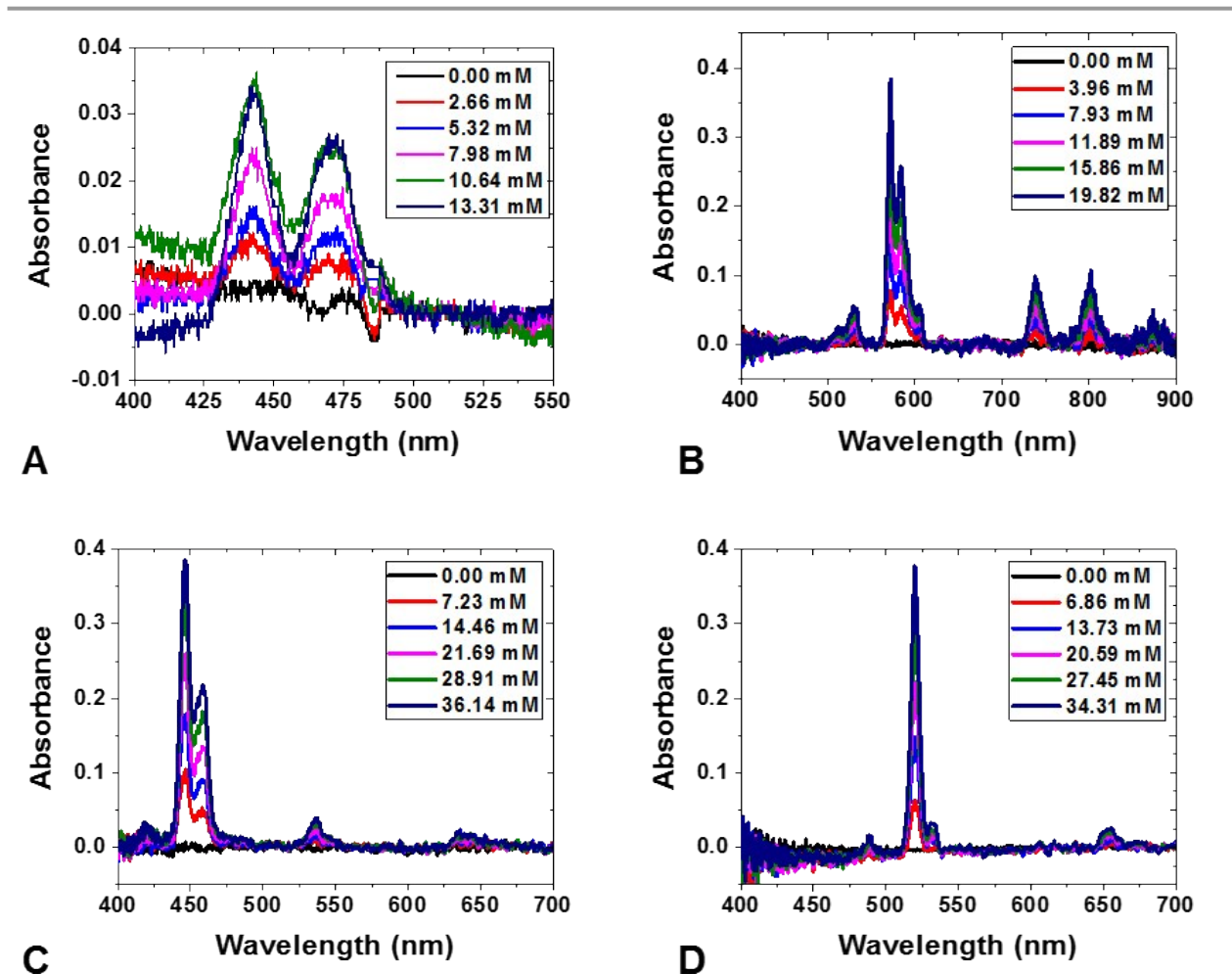
Figure 5: Spectra of lanthanides A) $Pr(NO_3)_3$ B) $Nd(NO_3)_3$ C) $Ho(NO_3)_3$ D) $Er(NO_3)_3$ in organic phase. Organic phase consisting 0.25 M HEH[EHP] in n-dodecane. Samarium and europium are not shown due to there being no useable peaks in their spectra.

Table 4: Molar absorptivity values calculated from Beer's law plots of representative wavelengths for each lanthanide in organic phase. Organic phase consisting 0.25 M HEH[EHP] in n-dodecane. Samarium and europium are not shown as there were no useable peaks in their spectra. Error is calculated using propagation of error from the uncertainty of the Beer's law plot slope.

Metal	Wavelength (nm)	Extinction Coefficient ($M^{-1}*cm^{-1}$)
Praseodymium	443	0.948 (±0.113)
Neodymium	572	7.74 (±0.06)
Holmium	446	4.27 (±0.18)
Erbium	520	4.47 (±0.06)

From these Beer's law plots the molar absorptivity of each lanthanide in each type of solution can be calculated. This is done based on Beer's law:

$$A = \varepsilon b c \tag{2}$$

With A = absorbance, ε = molar absorptivity, b = path length and c = concentration. Now with the y = mx+b of the line drawn from each Beer's Law plot with the y set as absorptivity and x set as concentration this leaves the ε*b equaling slope. Since the path length of the uv-vis probe is fixed at 2.5 cm in length the molar extinction coefficients can easily be calculated. The complete results for every wavelength fitted are shown in the appendices.

From these Beer's Law plots the limit of detection (LOD) could be calculated using:

$$LOD = \frac{3s}{m} \tag{3}$$

With m = slope of Beer's Law plot and s = standard deviation of the zero measurement. The results are shown in Table 5. It is noteworthy (but not surprising) that europium samples never had enough

distinguishable signal to give decent Beer's Law plots, thus no limit of detection could be calculated. For samarium the organic phase did not have enough distinguishable signal to get above the background noise, so its organic molar absorptivity also was not calculated.

Table 5: The limit of detection for the various lanthanides tested

Lanthanide	Aq λ (nm)	Aq LOD (mM)	Org λ (nm)	Org LOD (mM)
Pr	444	2.0	443	2.9
Nd	798	1.5	572	0.3
Sm	403	2.5	-	-
Eu	-	-	-	-
Ho	450	1.1	446	2.8
Er	520	1.1	520	0.8

Stirrer Speed Values:

Table 6: Kinetic results for variable stirrer speed tests. Aqueous phase was 0.96 M citric acid, 0.125M HEDTA and 0.0171 M $Nd(NO_3)_3$ at pH 2.52. Organic phase was 1 M HEH[EHP] in n-dodecane. Temperature was maintained at 25 °C.

Stirrer speed (rpm)	k_f (min^{-1})	log (k_f)	k_b (min^{-1})	log (k_b)
100	3.03 (±0.22) x 10^{-3}	-2.52	1.21 (±0.01) x 10^{-3}	-2.92
150	3.93 (±0.27) x 10^{-3}	-2.41	1.38 (±0.08) x 10^{-3}	-2.86
200	5.84 (±0.40) x 10^{-3}	-2.23	1.92 (±0.11) x 10^{-3}	-2.72
250	6.22 (±0.44) x 10^{-3}	-2.21	2.35 (±0.14) x 10^{-3}	-2.63
300	8.04 (±0.49) x 10^{-3}	-2.09	1.49 (±0.09) x 10^{-3}	-2.83
350	8.95 (±0.60) x 10^{-3}	-2.05	2.78 (±0.16) x 10^{-3}	-2.56
375	9.84 (±0.65) x 10^{-3}	-2.01	2.93 (±0.17) x 10^{-3}	-2.54
400	8.51 (±0.59) x 10^{-3}	-2.07	2.95 (±0.18) x 10^{-3}	-2.53
425	9.31 (±0.61) x 10^{-3}	-2.04	2.74 (±0.16) x 10^{-3}	-2.57
450	6.21 (±0.40) x 10^{-3}	-2.21	1.63 (±0.10) x 10^{-3}	-2.79

Table 7: Distribution results for variable stirrer speed tests. Aqueous phase was 0.96 M citric acid, 0.125M HEDTA and 0.0171 M $Nd(NO_3)_3$ at pH 2.52. Organic phase was 1 M HEH[EHP] in n-dodecane. Temperature was maintained at 25 °C.

Stirrer speed (rpm)	D	log (D)
100	2.51 (±0.09)	0.400
150	2.85 (±0.10)	0.455
200	3.04 (±0.10)	0.483
250	2.64 (±0.09)	0.422
300	5.41 (±0.17)	0.734
350	3.22 (±0.11)	0.508
375	3.35 (±0.11)	0.525
400	2.88 (±0.10)	0.460
425	3.40 (±0.11)	0.531
450	3.81 (±0.12)	0.581

References

1. W. T. Carnall, in Handbook of the Physics and Chemistry of Rare Earths, North-Holland Publishing Company, Argonne, IL, Editon edn., 1979, pp. 171-208.